

# Construction of Consistent Meson Exchange Currents by Laplace Transform<sup>†</sup>

Hartmuth Arenhövel and Michael Schwamb

*Institut für Kernphysik, Johannes Gutenberg-Universität, D-55099 Mainz, Germany*

(November 23, 2018)

We propose a new method for the construction of a consistent meson exchange current in  $r$ -space for the spin-isospin dependent central and tensor part of phenomenological nucleon-nucleon potentials by using a Laplace transformation, which allows the representation by a finite number of Yukawa functions. This method is applied to the Paris and the recent Argonne  $V_{18}$  potentials. Results are presented for electrodisintegration of the deuteron near threshold.

PACS numbers: 13.40.-f, 21.45.+v, 25.20.-x, 25.30.Fj

## I. INTRODUCTION

The contribution of meson exchange currents (MEC) to electromagnetic reactions (e.m.) on nuclei, like photo induced reactions and electron scattering, constitute an important manifestation of meson degrees of freedom mediating the strong interactions between nucleons in nuclei. They describe the e.m. interaction with a nucleus during the interaction of nucleons and appear formally in the nuclear current operator as two- or many-body operators. Thus they are intimately linked to the  $NN$ -interaction. However, for a given  $NN$ -potential there exists no a priori way of constructing the appropriate MEC-operators, unless the  $NN$ -potential is derived from an underlying more fundamental fieldtheoretical framework with explicit subnuclear degrees of freedom which allows the construction of the corresponding two-body currents in parallel to the  $NN$ -potential. Although the existence of exchange currents associated with an exchange  $NN$ -potential has been acknowledged for a long time, the early realistic potentials being phenomenological to a large extent prevented thus the explicit consideration of such exchange currents.

A breakthrough came with the meson-theory based construction of MEC-operators. Thus purely meson exchange models of the  $NN$ -interaction like the Bonn potentials [1] allow one to build the appropriate consistent MEC-operators uniquely (for a recent derivation including leading order relativistic contributions see [2]). In these studies it turned out that the most important MEC contributions came from the  $\pi$ - and  $\rho$ -MEC which are directly related to the spin-isospin dependent central and tensor part of the  $NN$ -potential [3–6]. But for largely phenomenological potentials the construction of a consistent MEC remained questionable. In view of the fact that realistic phenomenological potentials incorporated  $\pi$ -exchange as longest range contribution, one often used for such potentials only a regularized  $\pi$ -MEC as an approximation.

However, the above mentioned results for meson-theoretical models suggested a method which provides also for the spin-isospin dependent central and tensor part of a phenomenological potential a consistent MEC whose construction is based on an analogy with the properties of  $\pi$ - and  $\rho$ -MEC [7,8]. Essentially this method relies on a splitting of the spin-isospin dependent central and tensor part of a given  $NN$ -potential into a  $\pi$ - and  $\rho$ -like part for which the consistent MECs are known. While the approach of Riska [8] is based on the momentum space representation of the potential and can be applied to any given phenomenological potential, the method of Buchmann et al. [7] is conceived for  $r$ -space calculations and needs a representation of the potential as superposition of Yukawa functions. Thus the application of the latter method seems to be more limited because not all phenomenological potentials have such a form. On the other hand, in view of recent high precision, though largely phenomenological  $NN$  potentials, like the Argonne  $V_{18}$  [10], it would be desirable to have a method available which allows the construction of a consistent exchange current for such potentials directly in  $r$ -space representation.

It is the aim of the present brief note to show, that it is possible to represent a given realistic  $r$ -space potential in general as a superposition of Yukawa functions such that the construction of a consistent MEC in  $r$ -space is easily achieved. This new method is based on the representation of the radial central and tensor parts of a spin-isospin dependent potential by a Laplace transformation. First, we will briefly review in the next section the approaches of [7,8]. Sect. III contains the central idea introducing the Laplace transformation. Explicit applications to the Paris

---

<sup>†</sup>Supported by the Deutsche Forschungsgemeinschaft (SFB 443).

and Argonne potentials are presented in Sect. IV. In Sect. V we consider electrodisintegration of the deuteron near threshold as a test case for the evaluation of the corresponding MECs. Finally we close with a summary.

## II. BASIC FORMALISM

We will focus now on the spin-isospin dependent part of a given  $NN$ -potential having the general form

$$V^{\sigma\tau}(r) = \vec{\sigma}_1 \cdot \vec{\sigma}_2 \left( \vec{\sigma}_1 \cdot \vec{\sigma}_2 V_C^{\sigma\tau}(r) + S_{12} V_T^{\sigma\tau}(r) \right), \quad (1)$$

where

$$S_{12} = 3 \vec{\sigma}_1 \cdot \hat{r} \vec{\sigma}_2 \cdot \hat{r} - \vec{\sigma}_1 \cdot \vec{\sigma}_2 \quad (2)$$

denotes the usual spin tensor operator. A pure unregularized  $\pi$ -exchange potential is given by

$$V_\pi^{\sigma\tau}(\vec{r}) = \vec{\sigma}_1 \cdot \vec{\sigma}_2 \frac{3 V_\pi^0}{m_\pi^2} \vec{\sigma}_1 \cdot \vec{\nabla} \vec{\sigma}_2 \cdot \vec{\nabla} J_{m_\pi}(r), \quad (3)$$

with the potential strength denoted by  $V_\pi^0$  and

$$J_m(r) = \frac{e^{-mr}}{4\pi r}. \quad (4)$$

By recoupling

$$\vec{\sigma}_1 \cdot \vec{\nabla} \vec{\sigma}_2 \cdot \vec{\nabla} = \frac{1}{3} \left( \vec{\sigma}_1 \cdot \vec{\sigma}_2 \partial_{r,C}^2 + S_{12} \partial_{r,T}^2 \right) \quad (5)$$

with radial differentiation operators

$$\partial_{r,C}^2 = \frac{1}{r} \frac{d^2}{dr^2}(r \cdot) \quad \text{and} \quad \partial_{r,T}^2 = r \frac{d}{dr} \left( \frac{1}{r} \frac{d}{dr} \cdot \right), \quad (6)$$

and using

$$\partial_{r,C}^2 J_m(r) = m^2 J_m(r) - \delta(\vec{r}), \quad (7)$$

$$\partial_{r,T}^2 J_m(r) = m^2 F_T(mr) J_m(r), \quad (8)$$

with

$$F_T(x) = 1 + \frac{3}{x} \left( 1 + \frac{1}{x} \right), \quad (9)$$

it can be brought into the form (1) with

$$\begin{aligned} V_C^\pi(r) &= \frac{V_\pi^0}{m_\pi^2} \partial_{r,C}^2 J_{m_\pi}(r) \\ &= V_\pi^0 \left( J_{m_\pi}(r) - \frac{1}{m_\pi^2} \delta(\vec{r}) \right), \end{aligned} \quad (10)$$

$$\begin{aligned} V_T^\pi(r) &= \frac{V_\pi^0}{m_\pi^2} \partial_{r,T}^2 J_{m_\pi}(r) \\ &= V_\pi^0 F_T(m_\pi r) J_{m_\pi}(r). \end{aligned} \quad (11)$$

Analogously, the dominant part of the  $\rho$ -exchange potential has also the form (1) with

$$V_C^\rho(r) = 2 V_\rho^0 \partial_{r,C}^2 J_{m_\rho}(r) \quad \text{and} \quad V_T^\rho(r) = -V_\rho^0 \partial_{r,T}^2 J_{m_\rho}(r). \quad (12)$$

The potential strength is denoted by  $V_\rho^0$ .

The corresponding exchange currents read for  $\pi$ -exchange

$$\vec{j}_\pi(\vec{x}, \vec{r}_1, \vec{r}_2) = T_{12}^3 V_\pi^0 \left( \delta(\vec{x} - \vec{r}_1) \vec{\sigma}_1 \vec{\sigma}_2 \cdot \vec{\nabla}_2 J_{m_\pi}(|r_1 - r_2|) - (1 \leftrightarrow 2) \right. \\ \left. + \vec{\sigma}_1 \cdot \vec{\nabla}_1 \vec{\sigma}_2 \cdot \vec{\nabla}_2 J_{m_\pi}(|\vec{r}_1 - \vec{x}|) \overset{\leftrightarrow}{\nabla}_x J_{m_\pi}(|\vec{x} - \vec{r}_2|) \right), \quad (13)$$

and for  $\rho$ -exchange

$$\vec{j}_\rho(\vec{x}, \vec{r}_1, \vec{r}_2) = T_{12}^3 V_\rho^0 \left( \delta(\vec{x} - \vec{r}_1) (\vec{\sigma}_2 \times \vec{\nabla}_2) \times \vec{\sigma}_1 J_{m_\rho}(|r_1 - r_2|) - (1 \leftrightarrow 2) \right. \\ \left. + (\vec{\sigma}_1 \times \vec{\nabla}_1) \cdot (\vec{\sigma}_2 \times \vec{\nabla}_2) J_{m_\rho}(|\vec{r}_1 - \vec{x}|) \overset{\leftrightarrow}{\nabla}_x J_{m_\rho}(|\vec{x} - \vec{r}_2|) \right), \quad (14)$$

where we have introduced

$$T_{12}^3 = (\vec{r}_1 \times \vec{r}_2)_3. \quad (15)$$

Defining the currents in momentum space by

$$\vec{j}(\vec{q}, \vec{q}_1, \vec{q}_2) = \frac{1}{(2\pi)^3} \int d^3x d^3r_1 d^3r_2 e^{-i\vec{q} \cdot \vec{x}} e^{i\vec{q}_1 \cdot \vec{r}_1} e^{i\vec{q}_2 \cdot \vec{r}_2} \vec{j}(\vec{x}, \vec{r}_1, \vec{r}_2), \quad (16)$$

these currents read

$$\vec{j}_\pi(\vec{q}, \vec{q}_1, \vec{q}_2) = -i \delta(\vec{q} - \vec{q}_1 - \vec{q}_2) T_{12}^3 [\vec{\sigma}_1 (\vec{\sigma}_2 \cdot \vec{q}_2) v_\pi(\vec{q}_2) - (1 \leftrightarrow 2) \\ + \frac{\vec{q}_1 - \vec{q}_2}{q_1^2 - q_2^2} (\vec{\sigma}_1 \cdot \vec{q}_1) (\vec{\sigma}_2 \cdot \vec{q}_2) (v_\pi(\vec{q}_1) - v_\pi(\vec{q}_2))], \quad (17)$$

$$\vec{j}_\rho(\vec{q}, \vec{q}_1, \vec{q}_2) = -i \delta(\vec{q} - \vec{q}_1 - \vec{q}_2) T_{12}^3 [\vec{\sigma}_1 \times (\vec{\sigma}_2 \times \vec{q}_2) v_\rho(\vec{q}_2) - (1 \leftrightarrow 2) \\ + \frac{\vec{q}_1 - \vec{q}_2}{q_1^2 - q_2^2} (\vec{\sigma}_1 \times \vec{q}_1) \cdot (\vec{\sigma}_2 \times \vec{q}_2) (v_\rho(\vec{q}_1) - v_\rho(\vec{q}_2))], \quad (18)$$

where

$$v_{\pi/\rho}(\vec{q}) = \int d^3r V_{\pi/\rho}(r) e^{i\vec{q} \cdot \vec{r}} \quad (19)$$

denotes the corresponding Fourier transforms of the potentials.

As mentioned in the introduction, for the case of phenomenological central and tensor parts of a realistic spin-isospin dependent  $NN$ -potential, the construction of a consistent MEC is based on the idea to split these potential terms into a  $\pi$ -like and a  $\rho$ -like part for which the corresponding MEC are known. This method has been developed independently by Buchmann et al. [7] and Riska [8] for the Paris potential [9]. Buchmann et al. start from the representation of the Paris potential in terms of Yukawa functions which reads in particular for the spin-isospin dependent part

$$V_C^{\sigma\tau}(r) = \sum_{j=1}^{12} g_{C,j}^{\sigma\tau} J_{m_j}(r), \quad (20)$$

$$V_T^{\sigma\tau}(r) = \sum_{j=1}^{12} g_{T,j}^{\sigma\tau} F_T(m_j r) J_{m_j}(r). \quad (21)$$

Here  $m_j$ ,  $g_C^{\sigma\tau}$  and  $g_T^{\sigma\tau}$  denote appropriate masses and coupling constants (for details see [7]). Using (7) and (8) one finds

$$V_C^{\sigma\tau}(r) = \partial_{r,C}^2 \sum_{j=1}^{12} \frac{g_{C,j}^{\sigma\tau}}{m_j^2} J_{m_j}(r) + \left( \sum_{j=1}^{12} \frac{g_{C,j}^{\sigma\tau}}{m_j^2} \right) \delta(r), \quad (22)$$

$$V_T^{\sigma\tau}(r) = \partial_{r,T}^2 \sum_{j=1}^{12} \frac{g_{T,j}^{\sigma\tau}}{m_j^2} J_{m_j}(r) \quad (23)$$

These expressions can be rewritten as

$$V_C^{\sigma\tau}(r) = \partial_{r,C}^2 \left( V^{\pi-like}(r) + 2 V^{\rho-like}(r) \right) + \left( \sum_{j=1}^{12} \frac{g_{C,j}^{\sigma\tau}}{m_j^2} \right) \delta(\vec{r}), \quad (24)$$

$$V_T^{\sigma\tau}(r) = \partial_{r,T}^2 \left( V^{\pi-like}(r) - V^{\rho-like}(r) \right), \quad (25)$$

where the  $\pi$ - and  $\rho$ -like parts are given by

$$V^{(\pi/\rho)-like}(r) = \sum_{j=1}^{12} g_j^{\pi/\rho} J_{m_j}(r), \quad (26)$$

with coupling constants defined by

$$g_j^\pi = \frac{1}{3m_j^2} (g_{C,j}^{\sigma\tau} + 2g_{T,j}^{\sigma\tau}) \quad \text{and} \quad g_j^\rho = \frac{1}{3m_j^2} (g_{C,j}^{\sigma\tau} - g_{T,j}^{\sigma\tau}). \quad (27)$$

Thus the representation of the spin-isospin dependent part of the Paris potential in terms of  $\pi$ - and  $\rho$ -like potentials is achieved if the  $\delta$ -function disappears in (24), which means the coupling constants have to fulfil the following condition

$$\sum_{j=1}^{12} (g_j^\pi + 2g_j^\rho) = \sum_{j=1}^{12} \frac{g_{C,j}^{\sigma\tau}}{m_j^2} = 0. \quad (28)$$

If this condition is not fulfilled, as is the case for the Paris potential, one can modify in (20) the short range part of  $V_C^{\sigma\tau}(r)$  by splitting it into

$$V_C^{\sigma\tau}(r) = \tilde{V}_C^{\sigma\tau}(r) + V_C^{sr}(r) \quad (29)$$

such that  $\tilde{V}_C^{\sigma\tau}(r)$  is identical to  $V_C^{\sigma\tau}(r)$  in the long and medium range part but obeys (28). In [7] this is achieved by changing the coupling constant of the highest mass  $g_{C,12}^{\sigma\tau} \rightarrow \tilde{g}_{C,12}^{\sigma\tau}$ , where the latter is determined from (28), i.e. from

$$\tilde{g}_{C,12}^{\sigma\tau} = -m_{12}^2 \sum_{j=1}^{11} \frac{g_{C,j}^{\sigma\tau}}{m_j^2}. \quad (30)$$

The difference  $g_{C,sr}^{\sigma\tau} = g_{C,12}^{\sigma\tau} - \tilde{g}_{C,12}^{\sigma\tau}$  serves as coupling constant for  $V_C^{sr}(r) = g_{C,sr}^{\sigma\tau} J_{m_{12}}(r)$ . For the remaining short range potential  $V_C^{sr}$  a consistent MEC is easily constructed [7]. It is obvious that this procedure is not unique and that it introduces some ambiguity, which indeed is characteristic for such phenomenological approaches. The hope is that the important physics in the long and medium range part is preserved.

Riska on the other hand considers the momentum space representation of the potential terms obtaining the  $\pi$ - and  $\rho$ -like pieces from

$$v^{\pi-like}(p) = \frac{1}{3p^2} \left[ 4\pi \int dr r^2 \left( V_C^{\sigma\tau}(r) j_0(pr) + 2 V_T^{\sigma\tau}(r) j_2(pr) \right) - v_C^{\sigma\tau}(0) \right], \quad (31)$$

$$v^{\rho-like}(p) = \frac{1}{3p^2} \left[ 4\pi \int dr r^2 \left( V_C^{\sigma\tau}(r) j_0(pr) - V_T^{\sigma\tau}(r) j_2(pr) \right) - v_C^{\sigma\tau}(0) \right], \quad (32)$$

where the subtraction of the term

$$v_C^{\sigma\tau}(0) = 4\pi \int dr r^2 V_C^{\sigma\tau}(r) \quad (33)$$

is required in order to eliminate the  $\delta$ -function. It constitutes again a modification of the short range part of the original potential part as mentioned above. In fact, in this case it amounts to the subtraction of a  $\delta$ -function

$$V_C^{sr}(\vec{r}) = v_C^{\sigma\tau}(0) \delta(\vec{r}). \quad (34)$$

Also here the above mentioned ambiguity becomes apparent, because any finite range potential  $V_C^{sr}(r)$  with the property

$$4\pi \int dr r^2 V_C^{sr}(r) = v_C^{\sigma\tau}(0) \quad (35)$$

would also serve to eliminate the  $\delta$ -function.

The corresponding MECs are obtained from (13) and (14) by replacing the Fourier transforms  $v_\pi$  and  $v_\rho$  by the corresponding ones,  $v^{\pi-like}$  and  $v^{\rho-like}$ , respectively. This method appears more general than the approach of Buchmann et al. since it does not rely on the Yukawa representation. However, we now will show that also the latter method can be applied to potentials with a more general radial dependence.

### III. REPRESENTATION BY A LAPLACE TRANSFORM

Our first idea was to approximate the given potentials by a series of Yukawa functions whose coefficients and masses are obtained by a least square fit. But depending on the accuracy needed this can be quite a formidable task because of the high dimensional parameter space involved. But then it turned out that an easier and more systematic approach can be based on the representation of the potentials by a Laplace transform. Indeed, because of the fact that realistic potentials contain as longest range contribution a  $\pi$ -exchange potential, one can represent the central and tensor parts of a given realistic potential by a continuous superposition of appropriate Yukawa functions (compare with (20) and (21)), i.e.

$$\begin{aligned} V_C(r) &= \int_0^\infty dm g_C(m) J_{m+m_\pi}(r) \\ &= J_{m_\pi}(r) \int_0^\infty dm g_C(m) e^{-mr}, \end{aligned} \quad (36)$$

$$\begin{aligned} V_T(r) &= \int_0^\infty dm g_T(m) F_T((m+m_\pi)r) J_{m+m_\pi}(r) \\ &= \partial_{r,T}^2 J_{m_\pi}(r) \int_0^\infty dm \frac{g_C(m)}{(m+m_\pi)^2} e^{-mr}, \end{aligned} \quad (37)$$

which is essentially a Laplace transform representation. We note in passing, that the Fourier transform of  $V_C$  is simply given by

$$v_C(\vec{q}) = \int_0^\infty dm \frac{g_C(m)}{\vec{q}^2 + (m+m_\pi)^2}. \quad (38)$$

Introducing  $\pi$ - and  $\rho$ -like potentials as in (24) and (25) with corresponding representations

$$V^{\pi/\rho-like}(r) = \int_0^\infty dm g_{\pi/\rho}(m) J_{m+m_\pi}(r), \quad (39)$$

one obtains the following relations

$$V_C(r) = \int_0^\infty dm (g_\pi(m) + 2g_\rho(m)) \left( (m+m_\pi)^2 J_{m+m_\pi}(r) - \delta(\vec{r}) \right), \quad (40)$$

$$V_T(r) = \int_0^\infty dm (m+m_\pi)^2 (g_\pi(m) - g_\rho(m)) F_T((m+m_\pi)r) J_{m+m_\pi}(r). \quad (41)$$

Comparison with (36) and (37) gives

$$g_C(m) = (m+m_\pi)^2 (g_\pi(m) + 2g_\rho(m)), \quad (42)$$

$$g_T(m) = (m+m_\pi)^2 (g_\pi(m) - g_\rho(m)). \quad (43)$$

Again, in order to eliminate the  $\delta$ -function in (40), one needs the condition

$$\int_0^\infty dm (g_\pi(m) + 2g_\rho(m)) = \int_0^\infty dm \frac{g_C(m)}{(m+m_\pi)^2} = 0. \quad (44)$$

If this is not fulfilled, one has to separate again a short range potential as in (29)

$$V_C^{sr}(r) = \frac{1}{r} \int_0^\infty dm g_C^{sr}(m) e^{-(m+m_\pi)r}, \quad (45)$$

where the coefficients  $g_C^{sr}(m)$  in principle can be chosen quite arbitrarily except for the fulfilment of the relation

$$\int_0^\infty dm \frac{g_C^{sr}(m)}{(m+m_\pi)^2} = \int_0^\infty dm \frac{g_C(m)}{(m+m_\pi)^2}. \quad (46)$$

However, in practice one would choose them such that only the short-range part of the original potential is modified. The associated exchange currents read

$$\vec{j}_{\pi-like}(\vec{x}, \vec{r}_1, \vec{r}_2) = T_{12}^3 \int_0^\infty dm g_\pi(m) \left( \delta(\vec{x} - \vec{r}_1) \vec{\sigma}_1 \vec{\sigma}_2 \cdot \vec{\nabla}_2 J_{m+m_\pi}(|r_1 - r_2|) - (1 \leftrightarrow 2) \right. \\ \left. + \vec{\sigma}_1 \cdot \vec{\nabla}_1 \vec{\sigma}_2 \cdot \vec{\nabla}_2 J_{m+m_\pi}(|\vec{r}_1 - \vec{x}|) \overset{\leftrightarrow}{\nabla}_x J_{m+m_\pi}(|\vec{x} - \vec{r}_2|) \right), \quad (47)$$

$$\vec{j}_{\rho-like}(\vec{x}, \vec{r}_1, \vec{r}_2) = T_{12}^3 \int_0^\infty dm g_\rho(m) \left( \delta(\vec{x} - \vec{r}_1) (\vec{\sigma}_2 \times \vec{\nabla}_2) \times \vec{\sigma}_1 J_{m+m_\pi}(|r_1 - r_2|) - (1 \leftrightarrow 2) \right. \\ \left. + (\vec{\sigma}_1 \times \vec{\nabla}_1) \cdot (\vec{\sigma}_2 \times \vec{\nabla}_2) J_{m+m_\pi}(|\vec{r}_1 - \vec{x}|) \overset{\leftrightarrow}{\nabla}_x J_{m+m_\pi}(|\vec{x} - \vec{r}_2|) \right). \quad (48)$$

For the explicit application it is useful to discretize the integrals in (36) and (37), for example by Gauss quadrature

$$\int_0^\infty dm h(m) = \sum_{j=1}^N w_j h(m_j), \quad (49)$$

where  $N$  denotes the number of Gauss points,  $m_j$  the Gauss points and  $w_j$  the corresponding weights. Then one can represent the radial functions in (40) and (41) by a finite number of Yukawa functions

$$V_C(r) = \sum_{j=1}^N w_j (g_\pi(m_j) + 2 g_\rho(m_j)) \mu_j^2 J_{\mu_j}(r), \quad (50)$$

$$V_T(r) = \sum_{j=1}^N w_j \mu_j^2 (g_\pi(m_j) - g_\rho(m_j)) F_T(\mu_j r) J_{\mu_j}(r), \quad (51)$$

where we have set  $\mu_j = m_j + m_\pi$ . The consistent exchange current is then given as superposition of  $\pi$ - and  $\rho$ -like currents as listed in (13) and (14)

$$\vec{j}_{mec} = \vec{j}_{\pi-like}(\vec{x}, \vec{r}_1, \vec{r}_2) + \vec{j}_{\rho-like}(\vec{x}, \vec{r}_1, \vec{r}_2) \quad (52)$$

with

$$\vec{j}_{\pi-like}(\vec{x}, \vec{r}_1, \vec{r}_2) = T_{12}^3 \sum_{j=1}^N w_j g_\pi(m_j) \left( \delta(\vec{x} - \vec{r}_1) \vec{\sigma}_1 \vec{\sigma}_2 \cdot \vec{\nabla}_2 J_{\mu_j}(|r_1 - r_2|) - (1 \leftrightarrow 2) \right. \\ \left. + \vec{\sigma}_1 \cdot \vec{\nabla}_1 \vec{\sigma}_2 \cdot \vec{\nabla}_2 J_{\mu_j}(|\vec{r}_1 - \vec{x}|) \overset{\leftrightarrow}{\nabla}_x J_{\mu_j}(|\vec{x} - \vec{r}_2|) \right), \quad (53)$$

$$\vec{j}_{\rho-like}(\vec{x}, \vec{r}_1, \vec{r}_2) = T_{12}^3 \sum_{j=1}^N w_j g_\rho(m_j) \left( \delta(\vec{x} - \vec{r}_1) (\vec{\sigma}_2 \times \vec{\nabla}_2) \times \vec{\sigma}_1 J_{\mu_j}(|r_1 - r_2|) - (1 \leftrightarrow 2) \right. \\ \left. + (\vec{\sigma}_1 \times \vec{\nabla}_1) \cdot (\vec{\sigma}_2 \times \vec{\nabla}_2) J_{\mu_j}(|\vec{r}_1 - \vec{x}|) \overset{\leftrightarrow}{\nabla}_x J_{\mu_j}(|\vec{x} - \vec{r}_2|) \right). \quad (54)$$

In order to determine the unknown coefficients, one can choose an appropriate grid of  $N$  radial points  $r_i$  ( $i = 1, \dots, N$ ), and obtains an inhomogeneous set of  $2N$  linear equations for the  $2N$  coefficients  $g_\pi(m_j)$  and  $g_\rho(m_j)$

$$c_i = \sum_{j=1}^N A_{ij}^C (\pi_j + 2 \rho_j), \quad (55)$$

$$t_i = \sum_{j=1}^N A_{ij}^T (\pi_j - \rho_j), \quad (56)$$

where we have introduced for convenience

$$\begin{aligned} \pi_j &= g_\pi(m_j), & \rho_j &= g_\rho(m_j),, \\ c_i &= V_C(r_i)/J_{m_\pi}(r_i), & t_i &= V_T(r_i)/J_{m_\pi}(r_i), \\ A_{ij}^C &= w_j \mu_j^2 e^{-m_j r_i}, & A_{ij}^T &= w_j \mu_j^2 F_T(\mu_j r_i) e^{-m_j r_i}. \end{aligned} \quad (57)$$

It is worth mentioning that the matrices  $A_{ij}^C$  and  $A_{ij}^T$  do not depend on the potentials, only on the chosen grids of radial points  $r_i$  and masses  $m_j$ .

Solving the equations (55) and (56) by matrix inversion, one finds for the coefficients

$$\pi_j = \frac{1}{3} \sum_{i=1}^N \left( (A^C)_{ji}^{-1} c_i + 2 (A^T)_{ji}^{-1} t_i \right), \quad (58)$$

$$\rho_j = \frac{1}{3} \sum_{i=1}^N \left( (A^C)_{ji}^{-1} c_i - (A^T)_{ji}^{-1} t_i \right). \quad (59)$$

The condition (44) becomes

$$\sum_{j=1}^N w_j (\pi_j + 2 \rho_j) = 0. \quad (60)$$

If this is not obeyed for the given central potential, we split off a short range Yukawa potential for the highest mass  $\mu_N = m_N + m_\pi$

$$V_C^{sr}(r) = c \frac{e^{-\mu_N r}}{r}. \quad (61)$$

This means that the coefficients  $c_i$  in (58) and (59) have to be changed according to

$$c_i \rightarrow c_i + c e^{-m_N r_i}, \quad (62)$$

leading to new coefficients  $\pi_j$  and  $\rho_j$ . Then the unknown coefficient  $c$  is determined by the requirement that the resulting new coefficients  $\pi_j$  and  $\rho_j$  fulfil (60), which leads to

$$c = - \frac{\sum_{i,j=1}^N w_j (A^C)_{ji}^{-1} c_i}{\sum_{i,j=1}^N w_j (A^C)_{ji}^{-1} e^{-m_N r_i}}. \quad (63)$$

#### IV. APPLICATION TO PARIS AND ARGONNE $V_{18}$ POTENTIALS

As first example, we have chosen the Paris potential [9], because in this case we can compare the Laplace transform representation of the associated MECs directly with the consistent  $\pi$ - and  $\rho$ -like MECs of [7]. Since for a numerical evaluation one needs a reliable representation only for the radial range  $r = 0 - 10$  fm, we have chosen the grid of  $N$  radial points  $r_j$  in the range between 0 and about 12 fm with variable stepsize with the highest density of points close to the origin, where the potentials exhibit the largest variation, and then with increasing stepsize approaching the highest value  $r_N$ . In fact, an educated choice will have to take into account the radial behaviour of the potential under consideration. In detail, we have chosen the  $r$ -grid to be defined by the following expression

$$r_j = r_0 + (e^{a(j-1)} - 1) e^{b(j-1)} \text{ fm}, \quad (64)$$

with  $r_0 = 0.01$  fm,  $a = 0.01$ , and  $b$  is determined for a given  $N$  by the requirement that the highest point  $r_N$  lies approximately between 10 and 12 fm. The parameter  $b$  is listed in Tab. I. In order to check the convergence with respect to the number of points we have considered  $N = 12, \dots, 20$  in steps of 2. The Gauss points and weights for the integral over  $m$  have been chosen according to

$$m_j = s \tan\left(\frac{\pi}{4} x_j + 1\right), \quad (65)$$

$$w_j = \frac{\pi}{4} \frac{s y_j}{\cos^2\left(\frac{\pi}{4} x_j + 1\right)}, \quad (66)$$

where  $x_j$  and  $y_j$  are Gauss points and weights, respectively, for integration between  $-1$  and  $1$ . For a given  $N$  the scale factor  $s$  is determined by minimizing the mean absolute deviation between the Yukawa representation  $V^{(Y,N)}$  and the original potential  $V$

$$\Delta(V^{(Y,N)}) = \frac{1}{r_{max} - r_0} \int_{r_0}^{r_{max}} dr |V^{(Y,N)}(r) - V(r)|, \quad (67)$$

evaluated between  $r_0 = .01$  fm and  $r_{max} = 10$  fm. The resulting scale factors and the relative mean deviations, i.e.,  $\Delta(V^{(Y,N)})$  divided by the average potential strength  $|\bar{V}|$

$$|\bar{V}| = \frac{1}{r_{max} - r_0} \int_{r_0}^{r_{max}} dr |V(r)|, \quad (68)$$

for the central and tensor potentials are also listed in Tab. I.

In Fig. 1 we show the original central and tensor potentials together with their Yukawa representations where we have multiplied them by the inverse of the pion Yukawa function  $J_{m_\pi}(r)$  for  $N = 12, \dots, 20$  in order to exhibit in greater detail the accuracy of the representation. One readily notes the rapid convergence and the very good representation over the whole range for  $N \geq 16$ . Indeed, the Laplace transform representations for  $N = 18$  and 20 are undistinguishable from the original form on this scale. Therefore, we show in addition in Fig. 2 for  $N = 16, 18$ , and 20 the relative deviations of the Laplace transform representation from the original form. For small  $r$ -values up to about 3 fm the deviations are extremely small whereas for higher  $r$ -values the relative deviations become somewhat larger, but this is of little importance in view of the rapid fall-off of the potentials themselves with increasing  $r$ . It is interesting to note that the relative deviations are larger for the central part than for the tensor potential. The reason for this feature is the rather rapid variation of the central potential near the origin.

The analogous results for the Argonne  $V_{18}$  potentials are displayed in Fig. 3 and Fig. 4 with scale parameters and relative mean deviations listed in Table II. One readily notes again the excellent representation for  $N = 12, \dots, 20$ . In this case the relative deviations are larger in the tensor part, because the central potential exhibits a much smoother behaviour near the origin compared to the Paris potential. In fact, the Laplace transform representations of the central part for  $N = 18$  and 20 are undistinguishable from the original form in Fig. 3, and even on the magnifying scale of Fig. 4 one notes only very tiny deviations.

## V. RESULTS FOR DEUTERON ELECTRODISINTEGRATION NEAR THRESHOLD

A benchmark for the study of meson exchange current effects in electromagnetic reactions on nuclei is deuteron electrodisintegration near threshold at higher momentum transfers [2,11–14]. The threshold region is dominated by the  $M1$ -excitation of the antibound  $^1S_0$ -resonance in  $NN$ -scattering at very low energies. With increasing momentum transfer the inclusive cross section at backward angles, where the transverse current contribution via the inelastic transverse form factor dominates, the one-body current contribution drops rapidly due a destructive interference of deuteron  $S$ - and  $D$ -wave contributions. In this situation the contribution of MEC, which are of shorter range than the one-body currents, becomes relatively more important, in fact dominant. Only inclusion of such MEC gives a satisfactory description of experimental data yielding thus clear-cut evidence for the presence of exchange currents [4–6,11–14].

We show in Fig. 5 the backward inclusive cross section near threshold at a c.m. excitation energy of  $E_{np} = 1.5$  MeV as function of the momentum transfer squared, calculated for the consistent  $\pi$ - and  $\rho$ -like MEC according to [7] and for the new Laplace transform representation for  $N = 12, 16$  and 20. It is almost impossible to note a difference between the different curves on this scale. For this reason we exhibit in Fig. 6 the relative deviation between the Laplace transform representation for  $N = 12, 16$  and 20 and the original MEC of [7]. Already for  $N = 12$  the maximum deviation does not exceed 1 %, for  $N = 16$  it is less than 0.1 %. In fact, the difference to the  $N = 20$  result is hardly noticeable even on the enlarged scale of Fig. 6. For  $N = 20$  the agreement is perfect. This clearly demonstrates that one has achieved already with  $N = 12$  quite a satisfactory parametrization, while for  $N = 16$  an almost perfect description for the consistent MEC is obtained. Here, we do not compare to experimental data for which one would need to include additional contributions, because we only want to demonstrate that the new method works very well.

We then have evaluated the analogous MEC contributions for the Argonne  $V_{18}$  potential. Also in this case we found an excellent convergence of the Laplace transform representation as is demonstrated in Figs. 7 and 8 (note the further enlarged scale), where we show the same quantities obtained for the Argonne  $V_{18}$  potential as for the Paris potential. One readily notes that in this case the convergence is even more rapid. For  $N = 12$  the maximum deviation from the case  $N = 20$  is about 0.2 %, and for  $N = 16$  it is less than 0.01 %.

We will end this section with a comparison with experimental data. In Fig. 9 the theoretical results obtained for the Paris and the Argonne potentials are exhibited together with experimental data from Refs. [15–17]. The theory includes besides the consistent  $\pi$ - and  $\rho$ -like MEC in addition relativistic one-body current and wave function boost contributions of leading order in  $p/M$ . One readily notes a satisfactory agreement for both potential models with experiment up to a squared momentum transfer of about  $25 \text{ fm}^{-2}$ . At higher momentum transfers the theory deviates significantly from experiment. However, in this region one expects a break down of the present approach in view of the applied  $p/M$ -expansion [18].

## VI. SUMMARY AND OUTLOOK

In this note we have shown that it is possible to construct directly in  $r$ -space a consistent meson exchange current for a spin-isospin dependent  $NN$ -potential by representing the potential as a continuous superposition of Yukawa functions, essentially a Laplace transform representation. In this way it is possible to rewrite the potential into a  $\pi$ - and a  $\rho$ -like part, whose corresponding consistent MECs then serve as a basis for a consistent MEC for the given potential except for a small modification of the short range part.

The feasibility of this method by discretizing the continuous superposition into a finite number of Yukawa functions has been demonstrated first for the Paris potential for which a consistent  $r$ -space MEC exists already. For a given grid of  $N$  masses the corresponding coefficients of the Yukawa functions are uniquely determined by a properly chosen grid of  $N$  radial points and involve a simple matrix inversion only. It turned out that the convergence with the number of terms is very rapid, and that with  $N = 16$  one obtains an excellent representation of the potential. The same was found for the more recent Argonne  $V_{18}$  potential.

The resulting consistent MEC, represented by a corresponding superposition of  $\pi$ - and  $\rho$ -like MECs, has then be checked by evaluating the inclusive cross section of deuteron electrodisintegration near threshold. For the associated observable, the inelastic transverse form factor, which is sensitive to MEC, we found for the Paris potential excellent agreement with previous evaluations and for both potentials a very rapid convergence with the number of terms. Thus the present method will easily allow one to implement a consistent MEC into an  $r$ -space calculation using phenomenological  $NN$ -potentials.

Finally we would like to emphasize that, although consistency of the MEC with the potential is achieved, one has to be aware of the fact, that this MEC is by no means unique. We have already alluded to a certain arbitrariness in separating a short-range part in order to eliminate an otherwise appearing  $\delta$ -function. Furthermore, there is in addition a freedom in the spin-operator structure as has been pointed out already in [7]. Only the longest range part of the  $\pi$ -like exchange current, namely the genuine  $\pi$ -MEC is on safe grounds.

- [1] R. Machleidt, *Adv. Nucl. Phys.* **19**, 189 (1989).
- [2] F. Ritz, H. Göller, T. Wilbois, and H. Arenhövel, *Phys. Rev. C* **55**, 2214 (1997).
- [3] M. Chemtob, M. Rho, *Nucl. Phys.* **A163**, 1 (1971).
- [4] J.F. Mathiot, *Phys. Rep.* **173**, 63 (1989).
- [5] D.O. Riska, *Phys. Rep.* **181**, 207 (1989).
- [6] H. Arenhövel, *Few-Body Syst.* **26**, 43 (1999).
- [7] A. Buchmann, W. Leidemann, and H. Arenhövel, *Nucl. Phys.* **A443**, 726 (1985).
- [8] D.O. Riska, *Phys. Scrip.* **31**, 471 (1985).
- [9] M. Lacombe, B. Loiseau, J.M. Richard, and R. Vinh Mau, *Phys. Rev. C* **21**, 861 (1980).
- [10] R.B. Wiringa, V.G. Stoks, and R. Schiavilla, *Phys. Rev. C* **52**, 38 (1995).
- [11] J. Hockert, D.O. Riska, M. Gari, and A. Huffmann, *Nucl. Phys.* **A217**, 14 (1973).
- [12] J.A. Lock and L.L. Foldy, *Ann. Phys. (N.Y.)* **93**, 276 (1975).
- [13] W. Fabian and H. Arenhövel, *Nucl. Phys.* **A258**, 461 (1976).
- [14] B. Mosconi and P. Ricci, *Nuovo Cimento A* **36**, 67 (1976).
- [15] M. Bernheim, E. Jans, J. Mougey, D. Royer, D. Tarnowski, S. Turck-Chieze, I. Sick, G.P. Capitani, E. De Sanctis, and S. Frullani, *Phys. Rev. Lett.* **46**, 402 (1981).
- [16] S. Auffret *et al.*, *Phys. Rev. Lett.* **55**, 1362 (1985).
- [17] R.G. Arnold *et al.*, *Phys. Rev. C* **42**, R1 (1990).
- [18] G. Beck, T. Wilbois, and H. Arenhövel, *Few-Body Syst.* **17**, 91 (1994).

TABLE I. Parameter value  $b$  for the radial grid, scale parameter  $s$  for the mass grid of Gauss points and relative mean deviation for Paris potential as function of the number of Gauss points  $N$ .

$N$	12	14	16	18	20
$b$	0.42	0.34	0.29	0.245	0.21
$s$ [fm $^{-1}$ ]	1.64	2.20	2.67	3.09	3.48
$\Delta(V_C^{(Y,N)})/ \bar{V}_C $	$0.25 \cdot 10^{-4}$	$0.21 \cdot 10^{-5}$	$0.54 \cdot 10^{-6}$	$0.72 \cdot 10^{-7}$	$0.14 \cdot 10^{-7}$
$\Delta(V_T^{(Y,N)})/ \bar{V}_T $	$0.20 \cdot 10^{-3}$	$0.35 \cdot 10^{-4}$	$0.72 \cdot 10^{-5}$	$0.65 \cdot 10^{-6}$	$0.12 \cdot 10^{-6}$

TABLE II. Scale parameter  $s$  and relative mean deviation for Argonne  $V_{18}$  potential as function of the number of Gauss points  $N$ .

$N$	12	14	16	18	20
$s$ [fm $^{-1}$ ]	2.19	2.43	2.75	3.04	3.235
$\Delta(V_C^{(Y,N)})/ \bar{V}_C $	$0.21 \cdot 10^{-3}$	$0.69 \cdot 10^{-4}$	$0.58 \cdot 10^{-4}$	$0.45 \cdot 10^{-4}$	$0.36 \cdot 10^{-4}$
$\Delta(V_T^{(Y,N)})/ \bar{V}_T $	$0.61 \cdot 10^{-3}$	$0.24 \cdot 10^{-3}$	$0.11 \cdot 10^{-3}$	$0.31 \cdot 10^{-4}$	$0.98 \cdot 10^{-5}$

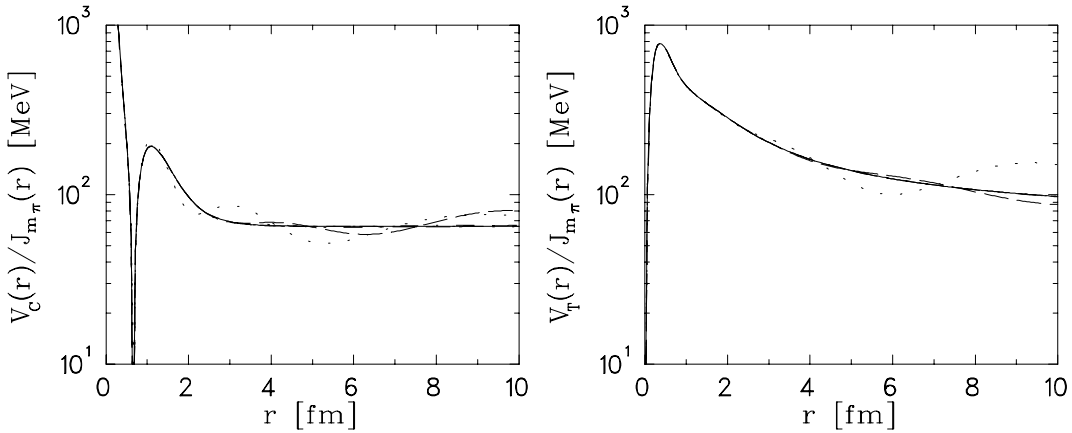


FIG. 1. Central and tensor spin-isospin dependent parts of Paris potential. Notation: original form: full curves, Laplace transform representation for different number  $N$  of Gauss points:  $N = 12$ : dotted,  $N = 14$ : dashed,  $N = 16$ : dash-dot.

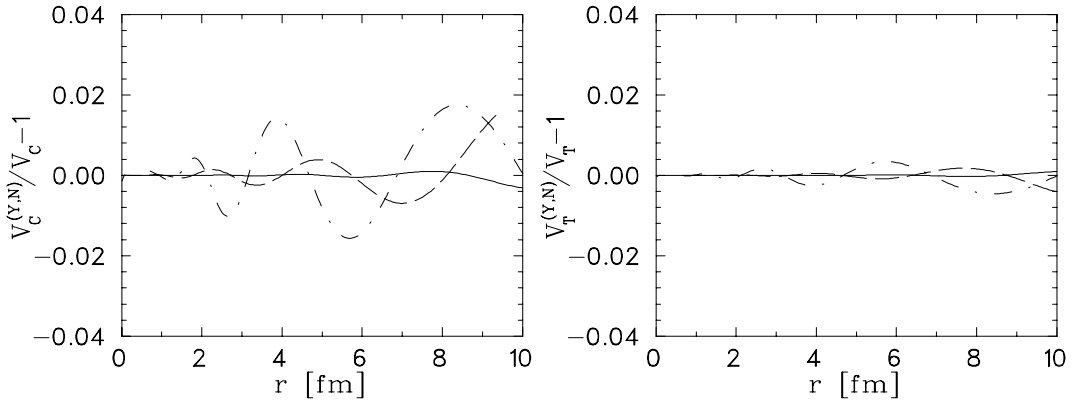


FIG. 2. Relative deviation of Laplace transform representation of central and tensor spin-isospin dependent parts of Paris potential from original form for different number  $N$  of Gauss points: Notation:  $N = 16$ : dash-dot,  $N = 18$ : long dashed,  $N = 20$ : full curves.

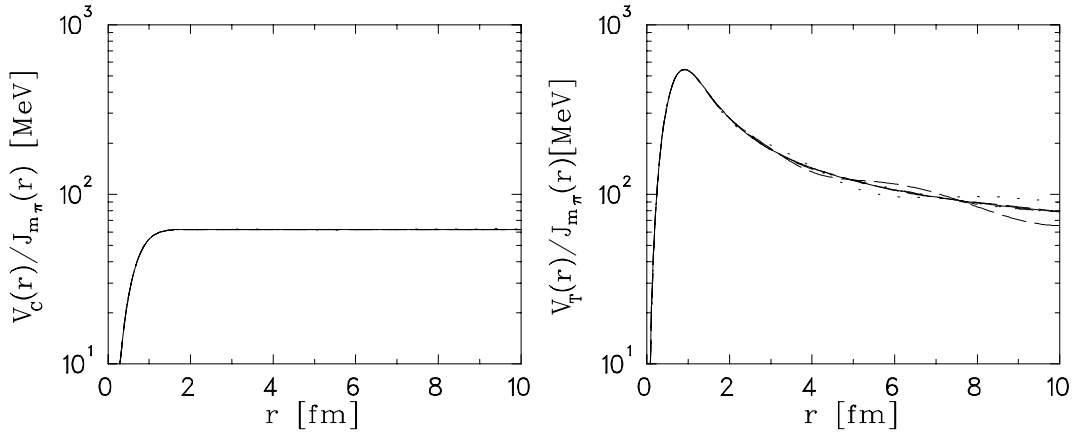


FIG. 3. Central and tensor spin-isospin dependent parts of Argonne  $V_{18}$  potential: original form and Laplace transform representation. Notation as in Fig. 1. In the central part the various Laplace transform representations are almost undistinguishable from original form.

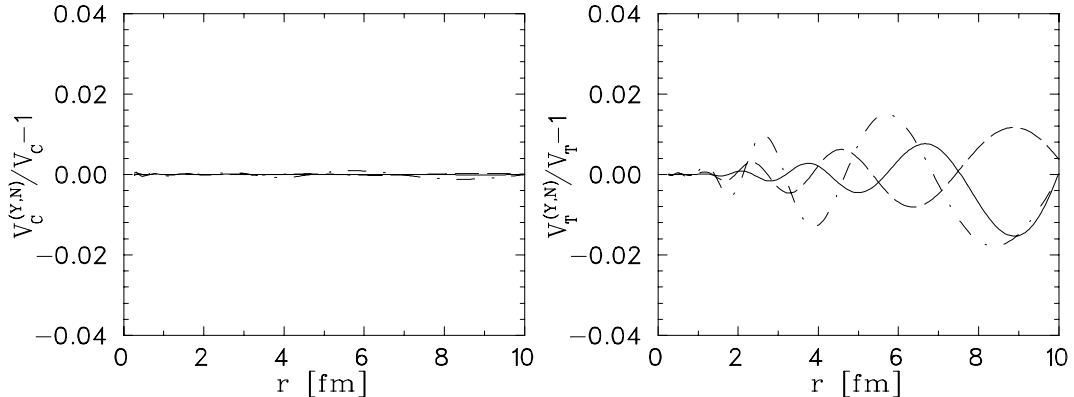


FIG. 4. Relative deviation of Laplace transform representation of central and tensor spin-isospin dependent parts of Argonne  $V_{18}$  potential from original form for different number  $N$  of Gauss points: Notation as in Fig. 2.

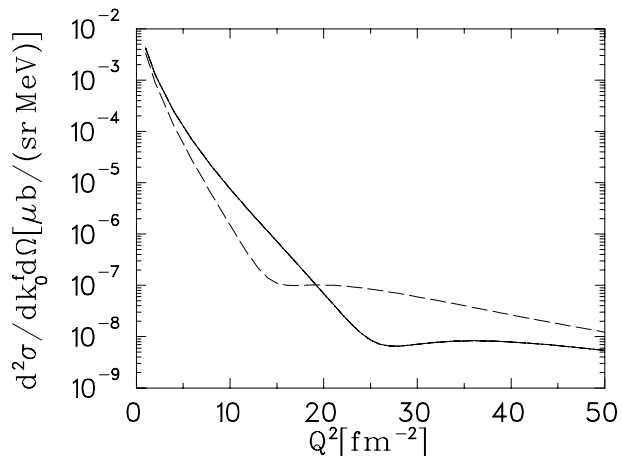


FIG. 5. Inclusive cross section for deuteron electrodisintegration near threshold for Paris potential for final state excitation energy  $E_{np} = 1.5$  MeV and electron scattering angle  $\theta_e = 155^\circ$ . Notation: solid curve: consistent MEC of [7] coinciding with consistent MEC of Laplace transform representations for  $N = 12, 16$  and  $20$ ; dashed curve: without MEC.

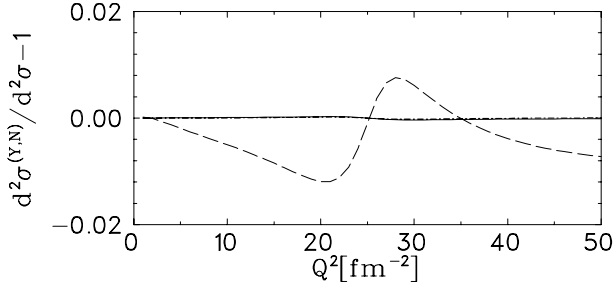


FIG. 6. Relative deviation of inclusive cross sections for deuteron electrodisintegration near threshold for Paris potential calculated with MEC from the Laplace transform representation ( $d^2\sigma^{(Y,N)}$ ) ( $N = 12, 16, 20$ ) to the one with MEC from [7] ( $d^2\sigma$ ) for final state excitation energy  $E_{np} = 1.5$  MeV and electron scattering angle  $\theta_e = 155^\circ$ . Notation of curves:  $N = 12$ : dashed,  $N = 16$ : dash-dot,  $N = 20$ : solid.

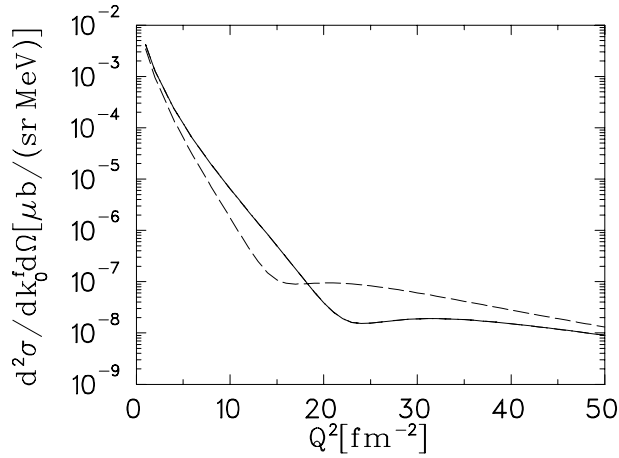


FIG. 7. Inclusive cross section for deuteron electrodisintegration near threshold for  $V_{18}$  potential for final state excitation energy  $E_{np} = 1.5$  MeV and electron scattering angle  $\theta_e = 155^\circ$ . Notation: dashed curve: without MEC; solid curve: consistent MEC of Laplace transform representations for  $N = 12, 16$  and 20, which coincide with each other.

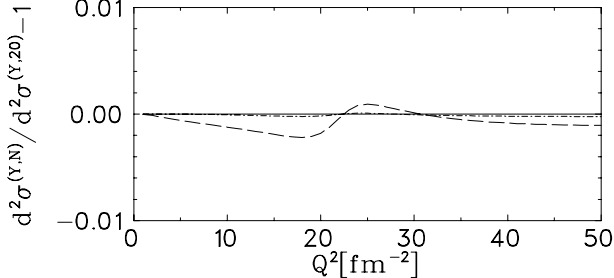


FIG. 8. Relative deviation of inclusive cross sections for deuteron electrodisintegration near threshold for  $V_{18}$  potential calculated with MEC from the Yukawa representation ( $d^2\sigma^{(Y,N)}$ ) for  $N = 12$  and 16 to the one with  $N = 20$  for final state excitation energy  $E_{np} = 1.5$  MeV and electron scattering angle  $\theta_e = 155^\circ$ . Notation as in Fig. 6.

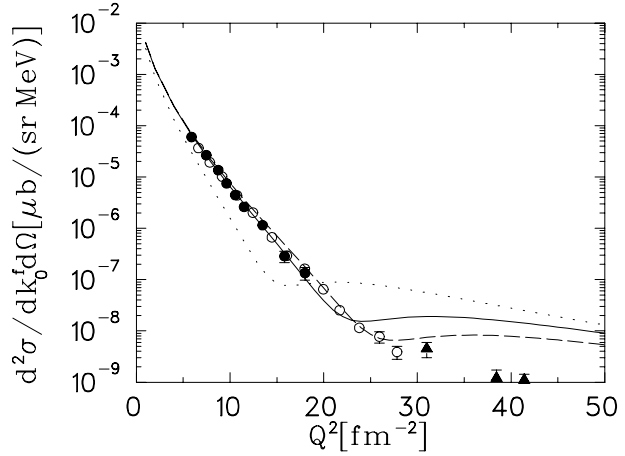


FIG. 9. Inclusive cross section for deuteron electrodisintegration near threshold for Paris and Argonne  $V_{18}$  potentials for final state excitation energy  $E_{np} = 1.5$  MeV and electron scattering angle  $\theta_e = 155^\circ$ . Notation: dotted curve: without MEC; solid curve: consistent MEC for Argonne  $V_{18}$  potential; dashed curve: consistent MEC for Paris potential; Experiment: filled circles: [15], open circles: [16] ( $\theta_e = 155^\circ$ , averaged over energies  $0 \text{ MeV} \leq E_{np} \leq 3 \text{ MeV}$ ); filled triangles: [17] ( $\theta_e = 180^\circ$ , averaged over energies  $0 \text{ MeV} \leq E_{np} \leq 10 \text{ MeV}$ ).